Techno-economic assessment of thermal energy storage technologies for demand-side management in low-temperature individual heating systems

Energy 236 (2021) 121496

Contents lists available at ScienceDirect

Energy

journal homepage: www.elsevier.com/locate/energy

Techno-economic assessment of thermal energy storage technologies for demand-side management in low-temperature individual heating systems

Yichi Zhang*, Pär Johansson, Angela Sasic Kalagasidis

Department of Architecture and Civil Engineering, Division of Building Technology, Chalmers University of Technology, Gothenburg, 412 96, Sweden

ARTICLE INFO

Article history:
Received 21 December 2020
Received in revised form
18 June 2021
Accepted 13 July 2021
Available online 16 July 2021

Keywords:
Thermal energy storage
Demand-side management
Water tank
Phase change material
Building thermal mass

ABSTRACT

The combined use of thermal energy storage (TES) technologies and heat pumps in building energy systems has been approved to achieve demand-side management. Although there is an increasing number of case studies about the TES applications, crosswise techno-economic evaluations of different technologies are rare, especially for applications in individual heating systems where the storage temperature range is less than 20 K. Hence, in this study, three TES options; water tank (WT), phase change material tank, and building thermal mass (BTM) are simulated and compared. A systematic analysis approach was proposed to assure impartial comparisons of the energy performance and the life-cycle costs (LCC). Special focus was paid on practical issues such as restricted charging power for different TES technologies. It was found that the majority of LCC savings arises from the peak load reduction. The study also shows that BTM is the most cost-effective TES technology while the WT is the least attractive option, due to larger heat loss and lower storage density. Moreover, less discharged energy and cost savings were found in well-insulated buildings due to the restricted discharging power. Still, there could be more incentives for household TES technologies if additional prices or policies are implemented.

1. Introduction

Following the Paris agreement on climate change, Nordic countries like Sweden and Denmark have set goals to cover 100% of their energy demand by renewable energy, with approximately 50% supplied from non-dispatchable sources such as wind and solar power [1]. With the increasing share of variable renewable energy (VRE) in the whole energy system, there is a growing need for flexibility measures to balance a mismatch between energy supply and demand.

In the meantime, thermal sector accounts for 50% of Europe's final energy consumption [2]. Due to a lack of district heating supply, and the need to upgrade conventional heating technologies, heat pumps were found to be one of the most promising heating sources for individual buildings, especially for single family houses (SFHs) [3]. In Sweden, nearly 60% of the SFHs already today have heat pumps (HPs) as a heating source in 2018 [4]. Thus, the idea of smart demand-side management (DSM) of heat pump and thermal energy storage (TES) in SFHs, which coordinates the dynamic energy supply and demand, has been developed to increase the share of VRE while providing flexibility to the electricity grid [5,6].

TES technologies applied in buildings are commonly grouped in sensible, latent, and thermal-chemical energy storage [7]. The widely recognized benefits of TES can be summarized into three points: (1) reduced investment and usage of peak capacity; (2) smoother operation of equipment and reduced running costs; (3) flexible load shifting to utilize non-dispatchable VRE or electricity with lower prices [8].

Apart from the prospected benefits, TES technologies also have certain limitations such as high investment cost and thermal losses. Therefore, several research papers were published in recent years, aiming to optimize the application of TES with the maximum benefit. A brief overview of these application studies in individual heating systems is summarized in Table 1. From the top-level application scenarios, the different energy sources and energy prices have significant influences on the benefits. In the studies restricted to one TES technology, the choice of optimization

* Corresponding author. Department of Architecture and Civil Engineering, Division of Building Technology Chalmers University of Technology 412 79, Gothenburg, Sweden.
E-mail address: yichi@chalmers.se (Y. Zhang).

https://doi.org/10.1016/j.energy.2021.121496

Nomenclature

Abbreviations

BTM	Building thermal mass
COP	Coefficient of performance
DHW	Domestic hot water
DHWT	Domestic hot water tank
DSM	Demand-side management
EC	Equivalent cycle
EH	Electric heater
GSHP	Ground source heat pump
HP	Heat pump
HTF	Heat transfer fluid
KPI	Key performance indicators
LCC	Life-cycle cost
NLP	Non-linear programming
O&M	Operation and management
PCM	Phase change material
REF	Reference
SEK	Swedish Krona
SFH	Single-family house
SH	Space heating
TES	Thermal energy storage
VRE	Variable renewable energy
WT	Water tank

Table 1
An overview of application studies of different thermal energy storage (TES) technologies applied in individual building energy systems for DSM. ASHP and GSHP represents air source heat pump and ground source heat pump, respectively.

TES	Case	Top-level scenarios		Bottom-level details		Ref
		Energy sources	Energy price	Heat loss	Storage delta T	
WT	SFH, Finland	GSHP	Variable	Yes	From 20 °C to 50 °C	[9]
WT	SFH, Germany	ASHP, PV, resistive heater	Variable	Yes	10 °C	[8]
WT	SFH, UK	ASHP, resistive heater, gas boiler	Two-rate	Yes	10 °C	[10]
PCM tank	SFH, UK	ASHP, resistive heater	Two-rate and variable	Yes	35 °C	[11]
BTM	SFH, Belgium	ASHP, PV	–	Yes	–	[12]
BTM	Apartment, Spain	ASHP, PV	Two-rate and variable	Yes	–	[13]
BTM	Apartment, Denmark	HP	Variable	Yes	–	[14]
WT&BTM	Building stock, Denmark	HP, wind power	Variable	Yes	15 °C	[15,16]
WT&BTM	Apartment, Italy	HP, PV, solar collector	Variable	Unclear	Unclear	[17]
WT, PCM&BTM	Office, Netherland	HP	Variable	No	75 °C	[18]

constraints and the obtained results are inevitably biased by chosen technology. Therefore, a generalized performance comparison of different TES technologies is well in need to assist the technological development in the future.

Optimization works were done to find out the economic and technical optimal design of WT [9–12], or combined design with BTM [15,16]. However, since different boundary conditions were applied, the achieved life-cycle economic benefit of WT ranges from negative [16] to as high as 13% [9]. Besides, for a typical SFH with a HP, the supply water temperature is kept lower than 60 °C to guarantee the overall HP efficiency [19]. Thus, the operating water temperature difference is often around 20 K, which restricts the utilization of sensible storage capacity and reduces the economic attractiveness [20]. Moreover, in terms of investment per unit storage capacity, the fixed part like the installation fee weigh more in small scale applications, which lowers the weights of storage material cost and reduces the economic attractiveness of the household WT [21]. In contrary, such investment of PCM tank remains relatively stable since a major part of it comes from material cost. Furthermore, only a small-scale investment of installing thermostats is needed to utilize BTM. In general, phase change material (PCM) tank and building thermal inertia (BTM) are less affected by the smaller temperature range.

As for the PCM, there are only limited studies on actively storing heat for DSM in low-temperature individual systems [11]. The case study of a smart building energy system in the U.K. has proved the potential benefits of PCM heat storage tank as a 20% reduction in end-user's electricity bill by active DSM. It is suggested that the varying benefits under different boundary conditions shall be further studied. Although the PCM tank still has limitations, such as the material fatigue and restricted discharging power [22], it could become a potential TES option in the future as the technology progresses and the manufacturing cost reduces.

The use of BTM has been acknowledged as a key technology to achieve DSM [23]. Compared to other active storage options, BTM has a simpler system design and less investment [16]. The control strategies and KPIs associated were reviewed in Ref. [24]. Based on the proposed methodologies, the performance and economic benefits of using BTM in single buildings [12,13,25–28] were evaluated. However, the occupants' willingness and acceptance of temperature changes often restrict the utilization [29].

Unlike from many studies dedicated to the single TES technologies, examples of cross-comparisons of different TES options in individual households are limited in the literature. The cost effectiveness of WT and BTM were studied at the whole Danish energy system level, showing that WT is, in general, less economic attractive than BTM due to high investment costs [15,16]. However, practical issues like low storage temperature range and restricted charge powers were not covered in these works, which might influence the delivered benefits of storage options. A detailed comparison of thermal performances of WT, PCM and thermochemical material can be found in Ref. [18], based on the theoretical assumption of the storage temperature as 90 °C. A systematic method to clearly identify and compare the benefits from different household TES options under realistic operation conditions is well in need, which can further enhance the understanding of TES options for DSM and help to make technical and economical optimal decisions.

For the purpose of addressing all relevant techno-economical details of the different TES technologies that are of interest for

DSM, in this study, a systematic analysis approach was proposed to evaluate the energy performance of the integrated system and breakdown the economic benefits from TES. Three TES options; WT, PCM tank, and BTM, were compared based on a typical Swedish SFH case with a ground source heat pump (GSHP) and a supplementary electric heater (EH) as the heating sources. The study aims to find the optimal system design and operation schemes with TES technologies to achieve the minimum life-cycle cost (LCC) over the project lifespan. To consider the effects of the building's thermal performance on the heat demand, three buildings with different level of insulation and thermal capacities were modelled. To quantify the possible influence on the LCC, different variables including operating schedules, TES sizes, and variable electricity prices are combined and investigated, formed into various scenarios. Based on the technical and economical performances of household TES options under these scenarios, the application areas for different TES options were defined.

2. Methodology

A recapitulative flowchart of the general methods applied in this study is shown in Fig. 1. Section 2.1 introduces the models for the heating system in the case building and the models for the three TES options. Then, the design and operation of the heating system with TES options were optimized to find the minimal life-cycle cost (LCC) over the project lifespan. Explanations of the optimization problems and constraints are presented in Section 2.2. The dynamic system performances were modelled and optimized under various scenarios, to investigate the possible influence from boundary conditions. The parameters for the analysis are explained in Section 2.3. The costs and benefits of different TES units were identified through comparisons between different scenarios. The methods to evaluate and compare the techno-economic performances are explained in Section 2.4.

2.1. System models

2.1.1. Heating demand and building models

A typical one-floor SFH with two residents, located in Gothenburg, Sweden, N 57° E 12°, is chosen for the case study. Gothenburg has a warm-summer humid continental climate to oceanic climate, with an average annual temperature of 7.7 °C. The case individual heating system contains a GSHP for baseload, an electric heater (EH) for peak load, TES options, a small domestic hot water tank (DHWT), transportation pipes and indoor radiators, as shown in Fig. 2.

The building has a total floor area of 80 m^2 and a total height of 3.6 m. The structures were derived from Ref. [30] and shown in Fig. 3, which represents a typical Swedish SFH built in the 1960s. Since the dynamic thermal performance of the building has significant influence on the BTM and flexibility, three buildings with different insulation levels and thermal capacities were modelled and compared. Table 2 presents the building component properties for the baseline SFH (SFH1) with a poor thermal insulation level, while the properties for the other two renovated SFHs are explained in Section 2.3 as design scenarios. An interior heat capacity of 0.13 MJ/(m^2.K) [31], which represents the capacity of indoor furniture and interior walls in the SFHs, was assumed for each building. The annual accumulated heating demand for SH and DHW in the baseline SFH1 are modelled as 201.9 kWh/m^2 and 24 kWh/m^2, respectively.

The modelling process of the building's energy performance is based on a previous thermal network model called ELAN [32], validated in Ref. [33]. In this model, each zone is simulated by a second-order network with two indoor temperature nodes which, for a multizone building, are linked by internal transmission and ventilation. The walls and other structures are partitioned into several layers according to their dynamic thermal properties to better represent the actual heat transfer and heat storage process. The model used a simplified method to calculate the radiative and convective heat transfer between interior surfaces and indoor air. The heat transfer to the ground is also simplified by a one-dimensional model, where a temperature boundary is given at the certain depth of 2 m. The temperature changes at this point can be found in the weather data. The ground between the building foundation and the temperature boundary is represented by several soil layers, with only vertical heat transfer process. The properties of these layers are derived from the thermal properties of the soil in Gothenburg.

Natural ventilation is considered in the building and the ventilation rate is set to be a constant value as 0.55 L/(s.m^2), which is slightly higher than the recommendation from Swedish building code [34], due to practical conditions in SFHs. Double-glazed, aluminum framed windows are applied, with a solar heat gain coefficient of 0.65.

The residents' occupancy and desired setpoint temperature are significantly influencing the building load profile [35]. Therefore, a stable schedule and a day schedule were investigated in this study. In the stable schedule, the temperature setpoint is kept at 20 °C and the internal heat gains from indoor equipment and residents' activities are kept stable at 10 W/(m^2·K) [36]. In the day schedule, there is a higher variability in the indoor air temperature between 7:00–19:00, shown in Fig. 4 (a), which represents a building that is occupied during the daytime. Correspondingly, there are also higher internal heat gains during daytime, see Fig. 4 (b), while the daily average internal heat gains is still kept at 10 W/(m^2·K). Based on the above-mentioned modelling methodology, the calculated heating demands are presented in Table 6.

Hydronic radiators are considered as indoor heat emitters, integrated into building models by applying a simplified one-dimensional air-water heat exchanger model. Explanations on the models can be found in Appendix A.1. By modelling the heat emitters and transportation pipes, the practical issues such as heat losses and thermal inertia of the equipment were considered, which improved the authenticity of the system models.

As for the DHW demand, the daily and monthly profiles are defined according to EN 15316:2007 [37,38], respectively. A 150 L domestic hot water tank (DHWT) is installed to keep the supply water temperature stable. A small heat exchanger as separation between the DHWT and the terminals is assumed, to prevent

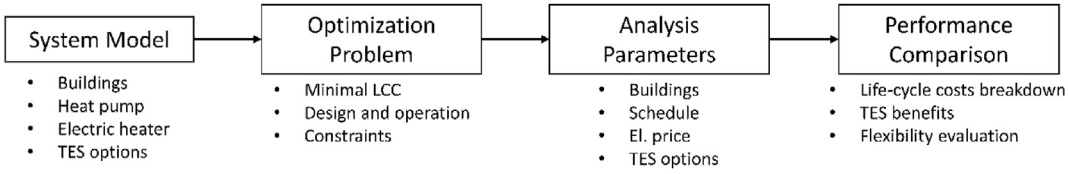

Fig. 1. Recapitulative flowchart of general methods applied in this study.

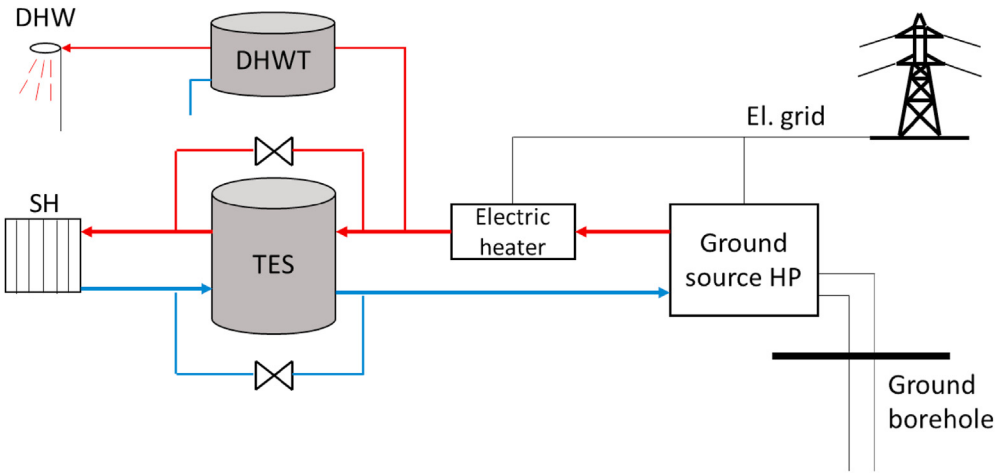

Fig. 2. Overview of the individual heating system integrated with TES technologies.

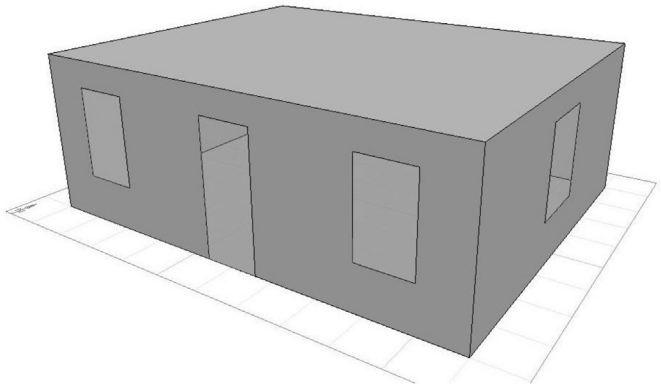

Fig. 3. Case single-family house model.

legionella issues. The temperature requirement for hot water tapping is around 45–50 °C for personal hygiene and dishwashing, as is considered in previous studies [39,40]. Thus, the control temperature of DHWT is set as 55 °C, to assure the satisfied hot water supply. Since the circulation pipes inside the SFHs are usually short [41], the sanitary temperature requirement for circulation flow is not considered in this study. The DHWT is modelled the same way as the WT designed in SH system, which is explained by Eqs. (2) and (3). Due to the intermittent nature of domestic hot water demand, the DHWT is not considered for the active demand response and optimization. A deterministic control strategy, that the charging process automatically starts when the temperature of the second top layer of DHWT is less than the setpoint temperature, is applied.

2.1.2. Heat source models

GSHP is one of the major heating sources for SFHs in Sweden [42] due to its relatively stable performance in cold climates. The coefficient of performance (COP) of GSHP is based on a simple regression model (Eq. (1)) [43]. The lift temperature is the temperature difference between the ground and the condenser outlet. While the outlet temperature is considered constant and equal to 55 °C, the ground source temperature is derived from the outdoor temperature profile, which has an average value of 10 °C. Then, the COP at the design condition is 3.5. The minimum operating load for HP is set to 20%, otherwise, the HP will be shut down.

$$COP = 8.77 - 0.15 \cdot T_L + 0.000734 \cdot T_L^2 \quad (-) \tag{1}$$

An auxiliary electric heater (EH) is designed in the system to save investment for peak capacity and to assure supply temperature for SH and DHW. The EH is assumed to have a 99% efficiency for generating heat. The design capacities of the GSHP and the EH are optimized to achieve the minimum LCC. The detailed descriptions about the optimization problem can be found in Section 2.2. The optimized sizes of heat sources in three investigated buildings are presented in Table 11.

In the baseline SFH1, the required heating power is 10 kW and the optimized installed capacities of the GSHP and EH are 4.2 kW and 5.8 kW, respectively. In total, the annual heat supply from the GSHP and EH are 16.5 MWh and 1.7 MWh. The EH is mostly used in the peak demand period, such as the morning and afternoon of the building during the winter, when it has higher temperature requirement but limited heating capacity of GSHP. Thus, one of the benefits of TES comes from shifting such peak demand into the period with available GSHP heating capacity, as is further illustrated in Section 3.1.

2.1.3. Thermal energy storage models

A one-dimensional vertically stratified WT model with 10 layers was used in this study, which has been commonly applied in several WT optimization studies [9,10]. The hot water is collected from the top while the cold return water enters the bottom. The

Table 2
Component properties for the baseline single-family house (SFH1) from Ref. [30].

Elements	Structure (from exterior to interior)	Thickness (mm)	U-value (W/m^2.K)	Heat capacity (MJ/K)
External wall	Concrete (60 mm), mineral wool (100 mm), Concrete (60 mm)	220	0.299	7.4
Roof	Mineral wool (130 mm), Concrete (220 mm)	350	0.214	7.1
Floor	Mineral wool (100 mm), Concrete (150 mm)	250	0.283	4.9
Window	Double-glazed, 4 mm + 20 mm+4 mm	28	2.5	–
Ventilation	Natural ventilation at 0.55 L/(s.m^2)	–	–	–

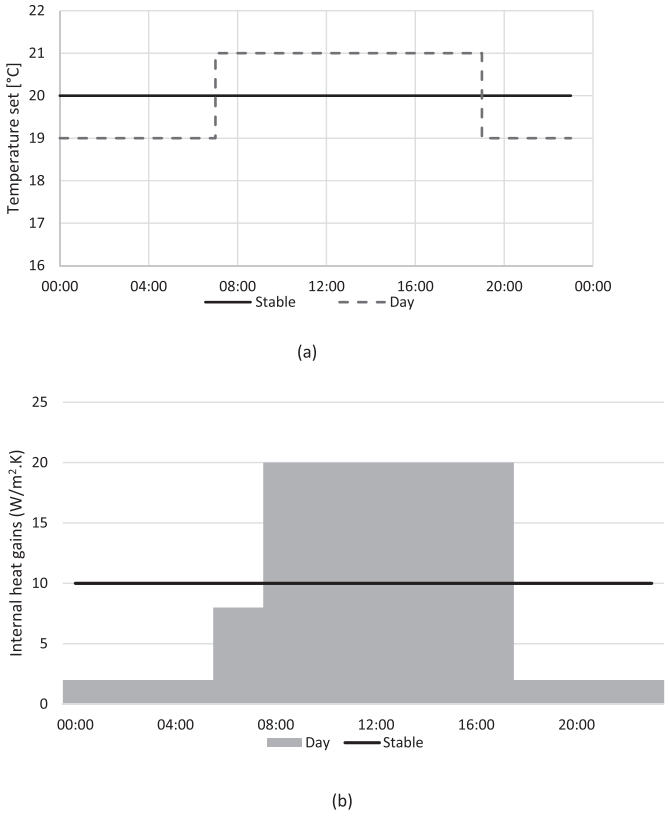

Fig. 4. Stable schedule and day schedule investigated in this study. a) Temperature setpoints; b) Internal heat gains.

energy balance equations are explained in Eqs. (2) and (3).

$$Q_{SOC,t} = Q_{SOC,t-1} + \left(\dot{Q}_{ch,t} - \dot{Q}_{dch,t} - \dot{Q}_{loss,t}\right) \cdot \Delta t \ (kWh) \tag{2}$$

$$\rho V C_p \frac{\partial T}{\partial t} = A_{cross}\lambda \frac{\partial^2 T}{\partial x^2} - u\rho C_p \frac{\partial T}{\partial x} - K_{loss,wt} A_{ext}(T - T_a) \quad (W) \tag{3}$$

where $Q_{SOC,t}$ (kWh) is energy stored at time t, calculated by the charging power $\dot{Q}_{ch,t}$ (W), discharging power $\dot{Q}_{dch,t}$ (W), and thermal losses $\dot{Q}_{loss,t}$ (kWh). x is the vertical coordinate. Water mass flowrate u (kg/s) is based on a control signal of the WT, which is consistent for all nodes. $K_{loss,wt}$ (W/(m^2·K)) is the heat loss factor of the WT, which is assumed to be 0.8 W/(m^2·K) according to a previous measurement study [44]. A_{cross} and A_{ext} (m^2) are the cross-sectoral and exterior surface area of each layer, respectively.

Due to limitations in the heat source efficiency, the charging and discharging temperature difference is 20 K, which generates an energy storage density of 23.3 kWh/m^3. In this study, 9 WT sizes, as presented in Section 2.3.2**,** were considered and compared to find the optimal design.

The PCM tank has a shell-and-tube storage structure where the heat transfer fluid (HTF) water is running through the pipes exchanging the heat with PCM, which is filling the shell space [45,46], as shown in Fig. 5. The model from Ref. [18], which uses a water pressure drop criterium to validate the feasibility of the TES tank design is applied in this study. The HTF tube coils inside the tank are represented by a one-dimensional straight tube, which is 20 m long and has an inner diameter of 8 mm. For simplicity of the simulation process, each HTF tube and surrounding layers of PCM are considered as a compartment and adiabatic boundaries are assumed between compartments. For each compartment, the PCM thickness is designed to be 15 mm.

The model for the HTF part is similar to the model of the WT but the heat loss function is moved to the exterior surface of the PCM tank. The model for the PCM part applies a one-dimensional representation for the heat conduction through the storage medium, shown in Eqs. (4) and (5). To simplify the modelling process, only heat conduction in the radial direction is considered [45]. Thus, the parameter x_{pcm} (m) denotes the maximum thickness of PCM layer. It is assumed that the PCM is isotropic and the natural convection during the melting process is neglected [47].

$$\rho V \frac{\partial \tilde{h}}{\partial t} = \lambda V \frac{\partial^2 T}{\partial x^2} + q_h, \quad 0 \le x \le x_{pcm}, \quad t \ge 0 \quad (W) \tag{4}$$

$$q_h = \begin{cases} K_{HTF} A_{HTF}(T_{HTF} - T_{PCM,x}), & x = 0 \\ K_{loss} A(T_{PCM,x} - T_a), & x = x_{pcm} \end{cases} \quad (W) \tag{5}$$

where q_h (W) encloses the heat transfer processes at the interior and exterior boundaries. K_{HTF} (W/(m^2.K)) denotes the heat transfer coefficient between the HTF and PCM layer [48]. K_{loss} is the heat loss factor of the PCM, which is assumed to be 0.5 W/(m^2·K) [11]. $\tilde{h}$ is the specific enthalpy, defined as

$$\tilde{h} = h_{ref} + \int_{T_{ref}}^{T} C_p dt + gL \quad (J/kg) \tag{6}$$

where h_{ref} (J/kg) is the enthalpy value at the reference temperature T_{ref} (°C), C_p (J/(kg·K)) is the specific heat capacity at temperature T (°C), L (J/kg) is the specific latent heat. g (−) is the liquid fraction function, which is used to update the phase-change status of the PCM, defined by a simple linear expression in Eq. (7). A certain type of paraffin wax [49] which melts at 44.8 °C, as presented in Table 3, was chosen as a PCM in this study.

$$g = F(T) = \begin{cases} 0, & T \le T_S, \ solid \\ \dfrac{T - T_S}{T_L - T_S}, & T_S \le T < T_L, \ transition\ state \\ 1, & T \ge T_L, \ liquid \end{cases} \quad (-) \tag{7}$$

2.2. Optimization problem

In the reference scenario without active load management through storage units, the heating power of the HP and EH are directly controlled by a proportional controller based on the calculated difference between the instantaneous indoor air temperature and the setpoint temperature from applied schedules. This scenario is also named REF scenario in the following analysis, as a baseline to other scenarios with DSM.

With the use of the TES units, the relatively expensive usage of the peak EH can be shifted to other periods when the GSHP is available. The system can adjust the load according to varying electricity prices for a lower operation cost. Thus, the system design and operation schemes are optimized to find the minimum life-cycle cost (LCC) of the heating system with a TES. Such results with DSM were compared with the results from REF scenario to identify the costs and benefits of TES units.

The overall objective function of the optimization problem is written in Eq. (8). The total LCC C_{tot} contains three parts: initial investment C_{inv}, annual cost for electricity C_{elop}, and annual

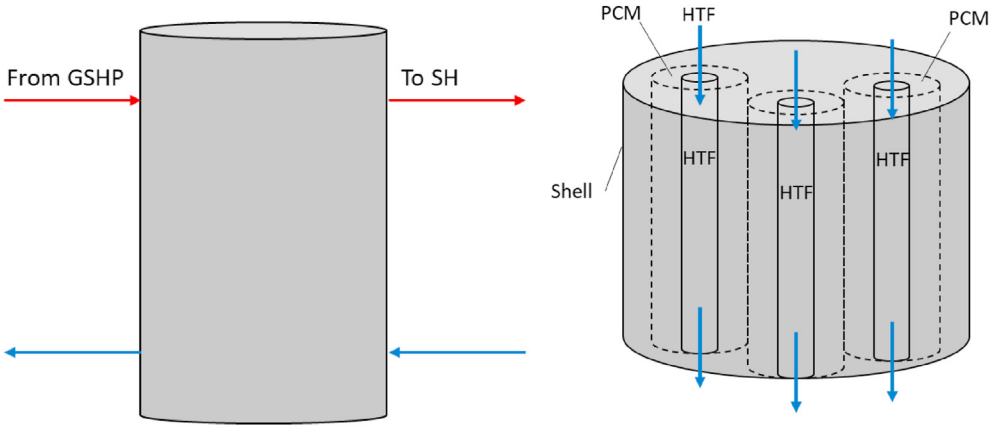

Fig. 5. Schematic of water tank (left) and phase-change material (PCM) tank (right).

Table 3
Chosen paraffin wax and its thermal properties [49].

Melting point (°C)	Solidification point (°C)	Latent heat (MJ/kg)	Density (kg/m^3)	Thermal conductivity (W/m·K)		Specific heat capacity (kJ/(kg·K))	
				Solid	Liquid	Solid	Liquid
44.8	45.2	223.5	834	0.358	0.148	2.2	1.8

operation and management (O&M) cost for equipment $C_{O\&M}$. Thus, the design sizes of the heat sources and TES units, and the operation schemes are all included as decision variables in the optimization problem. However, due to the non-linear characteristics of the integrated system, it is hard to find a global optimal result when incorporating both investment choices and annual operation schemes as variables. Thus, the higher-level optimal investment choices were manually found by performing and comparing parallel annual simulations. The investigated choices include the installed capacities of the GSHP and EH, and the sizes of TES units.

Then, the lower-level target of the optimization problem becomes the minimal annual operational electricity cost C_{elop}, as written in Eq. (9). More specifically, the decision variable becomes the charging and discharging operations of the TES units, to actively control the heating demand and adjust electricity usage.

$$\min C_{tot} = C_{inv} + \sum_{a=1}^{20} \frac{C_{elop} + C_{O\&M}}{(1+r)^t} \quad (\text{SEK}) \tag{8}$$

where a denotes the a-th year after investment. r is the nominal interest rate, which is set to 5%, considering the current interest rate in Sweden and the financial expectations of the SFH owners [50]. For each year, annual O&M cost $C_{O\&M}$ (SEK) is calculated as a ratio of the initial investment cost. The power consumption for water pumps and the control system is neglected in this study.

$$\min C_{elop} = \sum_{t=1}^{8760} C_{el,t} \cdot \left(\frac{Q_{HP,t}}{COP_t} + \frac{Q_{EH,t}}{\eta_{EH}} \right) \quad (SEK) \tag{9}$$

where $C_{el,t}$ (SEK/kWh) is hourly electricity price, $Q_{HP,t}$ and $Q_{EH,t}$ are the heating power for HP and EH at time t respectively.

To reduce optimization variables and reduce the calculation efforts, the annual optimization process is discretized into 365 daily optimizations [51]. The optimization length of one day is also reasonable considering the accuracy for forecasting the weather conditions and varying electricity prices. For each day, the hourly controls of the TES units are optimized for the lowest operational electricity cost. The system state at the end of each day becomes the starting state for the optimization in the next day. Thus, the optimization process becomes continuous but separated among different days. Then, the results from 365 days are summed altogether as the annual results. The above-mentioned optimization process is applied on a model predictive controller to control the detailed system, as shown in Fig. 6. Since the focus of this study is TES options for space heating, the DHWT is controlled with the deterministic strategy under all scenarios, as mentioned in Section 2.1.1. The whole year of 2019 is simulated to be consistent with historical weather data. The simulation time step for the whole system is set to 1 s to numerically solve heat and mass transfer equations.

Several constraints for the decision variables and system states were included to guarantee a practical meaning of the system operation. The HP should be operated within the possible range of its maximum heating power:

$$0.2 \le \frac{Q_{HP,t}}{Q_{HP,max}} \le 1 \; or \; Q_{HP,t} = 0 \tag{10}$$

For each day as an optimization cycle, the energy balance for WT and PCM holds:

$$\sum_{t=0}^{23} \left(\dot{Q}_{ch,t} - \dot{Q}_{dch,t} - \dot{Q}_{loss,t} \right) \cdot \Delta t \ge 0 \quad (kWh) \tag{11}$$

For solving the above non-convex global non-linear optimization problem (NLP), a mesh adaptive algorithm solver NOMAD [52], implemented in the MATLAB optimization toolbox OPTI [53], was applied. The optimization was solved on a ten-core Intel i9-9900 × 3.50 GHz CPU with 64 GB physical memory.

As for the detailed parameters used for the economic analysis, it shall be noted that the practical lifespan differs between projects and an example value of 20 years is applied in this study. The parameters of investment and annual O&M cost for equipment in this study are presented in Table 4. The currency used in this study is

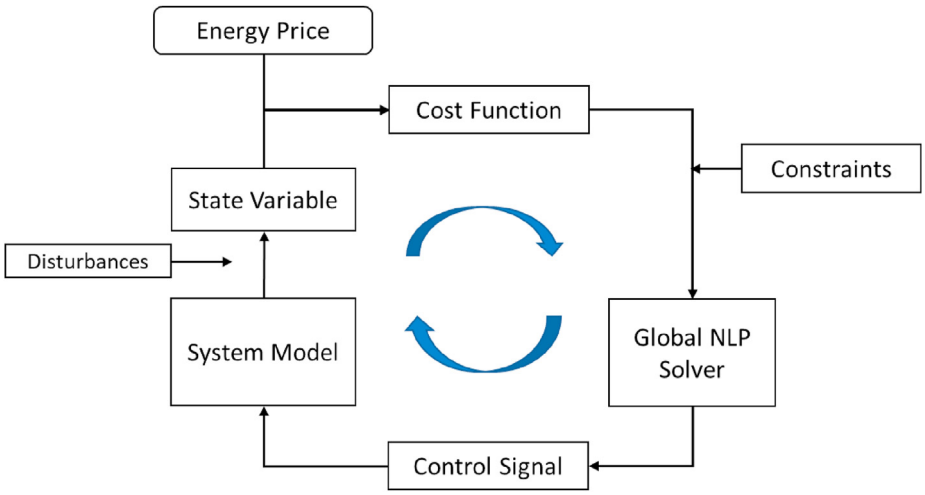

Fig. 6. Framework of model predictive control.

Table 4
Investment and annual O&M cost for equipment.

Equipment/capacity unit	Lifetime (years)	Fixed (SEK)	Specific (SEK/unit capacity)	O&M	Reference
GSHP/kW[a]	20	20,000	15,000	1%	[54]
EH/kW	10	–	500	1%	[8]
WT[b]/m^3	20	–	16,800	0%	[21]
PCM tank[c]/m^3	20	–	21,600	0%	[55]
Thermostats/household	20	–	2500	0%	[16]

[a] Investment for borehole is included.
[b] Investment for WT varies drastically with its size [21]. The value used here refers to the WT smaller than 1 m^c.
[c] Compact storage unit size including tubes and gaps between compartments.

Swedish Krona (SEK), which equals to on average 0.095 euro for the year of 2019. During the 20 years of operation, it is assumed that the EH needs to be reinvested once due to its short lifetime.

2.3. Analysis parameters

This section introduces the key parameters that were investigated in this study, which are the building physics and TES sizes from inside of the system and the variable electricity prices from outside of the system. Based on them, a combination of parameters is chosen for every scenario, and the TES performances were compared. The flowchart summarizing the parameters and relationships is presented in Fig. 7.

2.3.1. Buildings

Based on the same building structure as the baseline SFH1, the SFH2 with improved insulation levels, and a newly built building, SFH3, were also investigated in this study. The renovation measures and building properties were created according to TABULA [30] and investigations of Swedish passive houses [56]. Table 5 explains the detailed component parameters and Table 6 summarizes the heat capacities of the three case buildings.

2.3.2. TES options

For the WT and PCM tank, the storage size is influencing the available storage capacity and economic benefit. As illustrated in Section 2.2, the best investment choices were manually acquired by

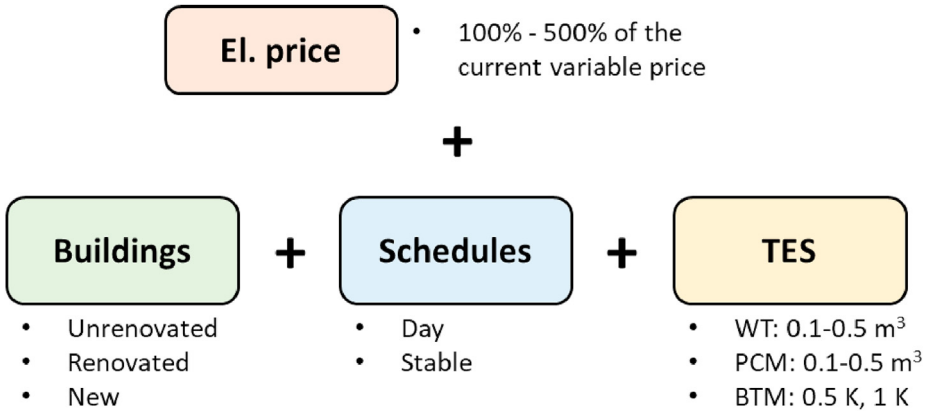

Fig. 7. Flowchart of the investigated key parameters and scenarios.

Table 5
Component properties for the insulation-improved single-family house (SFH2) and newly built SFH3.

Building	Elements	Structure (adding to exterior side)	Thickness (mm)	U-value (W/m^2·K)
SFH2 (Improved insulation)	External wall	SFH1 +mineral wool (200 mm)	420	0.125
	Roof	SFH1 +mineral wool (250 mm)	600	0.09
	Floor	SFH1 + EPS board (200 mm)	450	0.15
	Window	Triple-glazed 4 + 12+4 + 12+4 mm	36	0.8
	Ventilation	Natural ventilation at 0.55 L/(s.m^2)	–	–
SFH3 (Newly built)	External wall	SFH1 +mineral wool (300 mm)	520	0.092
	Roof	SFH1 +mineral wool (500 mm)	850	0.06
	Floor	SFH1 + EPS board (200 mm)	450	0.15
	Window	Triple-glazed 4 + 12+4 + 12+4 mm	36	0.8
	Ventilation	Natural ventilation at 0.3 L/(s.m^2)	–	–

Table 6
Heating demand, heat capacity, and time constant of the case single-family houses (SFHs).

Buildings	Heating demand (kWh/m^2)		Heat capacity (kWh/K)		Heat loss (W/K)	Time constant (h)	
	SH	DHW	Total	Interior		Total	Interior
SFH1	201.9	24.0	8.4	3.0	140.1	59.9	21.4
SFH2	93.8	24.0	10.2	3.0	94.5	108.3	31.8
SFH3	36.1	24.0	11.7	3.0	59.7	195.8	50.3

running parallel simulations and the resulting WT and PCM tank sizes are summarized in Table 7. Since the design storage temperature range for the WT is limited to 20 K, the WT has low storage density compared to the PCM tank and the investment per storage capacity becomes accordingly larger.

As for the system utilizing the BTM, two temperature deviations from the setpoint temperature, 0.5 K, and 1 K, were considered, as thermal comfort acceptance of residents during DSM control. The former value is derived from a field measurement of building flexibility control in Gothenburg [29]. The latter value is due to the requirement of indoor comfort from ISO 7730:2005 [57]. The average temperature for each day is controlled to the setpoint temperature to avoid a permanent decrease in thermal comfort. Otherwise, the controller will reduce the energy use and operation cost directly. This refers to an energy-saving measure which deviates from the objective of this research. In contrast, the indoor air temperature in the WT and PCM tank systems were controlled strictly to the setpoint temperature.

2.3.3. Electricity prices

The electricity price in Sweden comprises two parts, the fixed part, and the variable part. The former is decided by the tax, network prices, and other local factors and the latter comes from NordPool spot market [58]. The average electricity price during 2019 is 1.522 SEK/kWh whereof 33% is the variable part. To investigate the influence of the variable prices, four extra price patterns were generated by amplifying the variable difference, while keeping the average price fixed. The current price pattern is named 100% price and the new price patterns are named 200%–500% prices based on how much the variable part is amplified. The key parameters of the prices are summarized in Table 8.

Table 8
Parameters of the price patterns. Unit: SEK/kWh.

Price patterns	100%	200%	300%	400%	500%
Annual average	1.522	1.522	1.522	1.522	1.522
Max	2.418	2.807	3.196	3.585	4.012
Min	1.017	0.582	0.094	−0.395	−0.883
Average daily difference	0.203	0.405	0.608	0.810	1.013

2.4. Evaluation indexes

2.4.1. Flexibility

In this study, we applied the storage capacity and storage efficiency of a TES as indicators. For the BTM system, the charged and discharged capacity is calculated as the accumulated difference of heating powers between the optimal controlled TES system and REF scenario without DSM. Then, the storage efficiency η_{TES} is defined in Eq. (12).

$$\eta_{TES} = \frac{Q_{discharged}}{Q_{charged}} \quad (-) \tag{12}$$

2.4.2. Breakdown analysis of LCC saving

As mentioned above, the benefit of TES can be summarized into three points: peak reduction, smooth operation, and load shifting according to varying prices [8]. It has been proved that the smooth operation has rather small influence on household HPs compared to the occasions with large-scale HPs [59]. Thereby, since the focus is on household heating systems, such benefit from smooth operation is neglected. The limitation regarding the considered benefits is further discussed in Section 4. Then, a breakdown analysis of LCC saving C_{cs} is conducted for each scenario to quantify the benefit from installing TES:

$$C_{cs} = C_{PR} + C_{LS} - C_{loss} - C_{inv,TES} = C_{tot,REF} - C_{tot,TES} \quad (\text{SEK}) \tag{13}$$

where C_{PR} is the benefit from peak reduction, C_{LS} the benefit from load shifting, C_{loss} the equivalent cost due to heat losses, C_{inv} the additional investment for TES options.

The peak usage of the EH is substituted by the HP in non-peak hours, therefore the benefit from peak reduction is:

Table 7
Design parameters of water tank (WT) and phase-change material (PCM) tank.

TES	Volume (m^3)	Short name	Capacity (kWh)	Daily loss (kWh)	Storage density (kWh/m^3)
WT	0.1–0.5 step increase 0.05	WT-100 to WT-500	2.3–11.6	0.7–3.5	23.2
PCM	0.1–0.5 step increase 0.1	PCM-100 to PCM-500	5.6–28.2	0.2–1.1	56.5

$$C_{PR} = f \cdot \sum_{t=1}^{8760} C_{el,t} \cdot (Q_{EH,REF,t} - Q_{EH,TES,t}) \left(1 - \frac{1}{COP_{avg}}\right) \quad (SEK) \tag{14}$$

where f is the annuity to convert annual cost to LCC, calculated as:

$$f = \sum_{a=1}^{20} \frac{1}{(1+r)^t} \quad (-) \tag{15}$$

The equivalent cost due to thermal losses is calculated daily, according to each charging and discharging cycle and the daily average electricity price $C_{el,d}$.

$$C_{loss} = f \cdot \sum_{d=1}^{365} \left(Q_{charged,d} - Q_{discharged,d}\right) \cdot C_{el,d} \quad (SEK) \tag{16}$$

For any scenario with TES units, the LCC saving C_{cs} is directly calculated by comparing the LCCs of the TES scenario and REF scenario, as shown in the right part of Eq. (13). Then, the benefit from peak reduction C_{PR}, and the costs and investments can also be directly calculated based on above-mentioned methods. Since the specific price difference for each shifted load is hard to be traced, the benefit from load shifting C_{LS} (SEK) is calculated indirectly by subtracting other known parts from the total cost saving C_{cs} (SEK).

3. Results

3.1. SFH1 under day schedule

The annual electricity consumptions and LCC for SFH1 systems operated under the day schedule are shown in Fig. 8. As explained earlier, the usage of EH is caused by the limited heating capacity of GSHP during the peak demand period, such as the cold winter days. As a result, the high initial investment for HPs is reduced. For the REF scenario, the maximum heating load is 10 kW while the minimum LCC is achieved when the installed heating power of heat pump is 4.2 kW. The minimum LCC is 2830 SEK/m^2, which is 639 SEK/m^2 less than the option where the HP is the only heat source. In the minimal LCC case, the annual heat generation from the EH is 1732 kWh, which is 9.5% of the total demand. The actual electricity consumption is 6444.4 kWh per year, which is 1271 kWh more than the option without the EH.

With the installations of TES units, the available heating capacity of the HP during off-peak period can be charged inside the TES and discharged during the peak demand period. Thus, the original usage of the EH in REF scenario can be further shifted to the usage of HP, which has much lower operational costs. The TES units maximize the usage of the HP. The annual performances of three example TES units are also shown in Fig. 8. Compared to the WT with a same design volume, the PCM tank has larger storage capacity and can thus reduce more usage of the peak EH. The maximum allowable active temperature deviation is assumed as 1.0 K to utilize the BTM. Although the BTM system has larger peak electricity consumption than PCM system, the LCC is lower due to the relatively small investment for the use of BTM.

To exemplify the peak reduction benefit, the power duration curves of the EH for the above typical systems are shown in Fig. 9. The hourly powers are sorted from the largest to the smallest and are drawn on the figure. The time-axis represents the scattered hours corresponding to the sorted powers and are, therefore, not continuous in real time-horizon. The presented curves are in accordance with the annual results in Fig. 8. The EH is used for approximately 1500 h in the REF scenario and the reductions of its usage by TES units are mostly happening in the first 1000 h. However, the peak reduction benefit is not working in the highest load period since this period refers to the sequence of the coldest 50 h of the year when all equipment is operating at their maximum capacity. In other words, there is no extra capacity in the system for the peak load to be shifted. The PCM system has the best peak reduction benefit while the WT system and BTM system has similar benefits.

The above analysis is only limited in specific TES sizes. To quantify the possible influence on the cost-savings, the LCC saving rate of the TES systems under different storage options and price patterns were simulated and presented in Fig. 10. Note that the LCC saving rate is calculated according to the difference of LCC between the REF scenario and the TES scenario, while the WT and PCM are named according to their volume (see Table 7). As the variable part of the price is increasing, the LCC saving rate becomes larger. The highest LCC saving for the WT and PCM tank is achieved at the volume of 200 L and 100 L, respectively, while a further increment of their storage volume decreases the economic benefit. It is also evident that the PCM system has better economic performance than the WT system. For the BTM system, the LCC saving is highly dependent on the temperature deviation. A strict temperature range of 0.5 K generates a cost-saving rate of 1.6% at the current energy price, while the range of 1 K has the largest cost-saving rate among all investigated TES options. Similar findings that the WT is less economically attractive compared to BTM is also provided in Ref. [15].

To further investigate the reasons behind the different economic benefits, Fig. 11 presents the breakdown analysis of LCC saving for typical scenarios. The cost saving derives mainly from the reduced

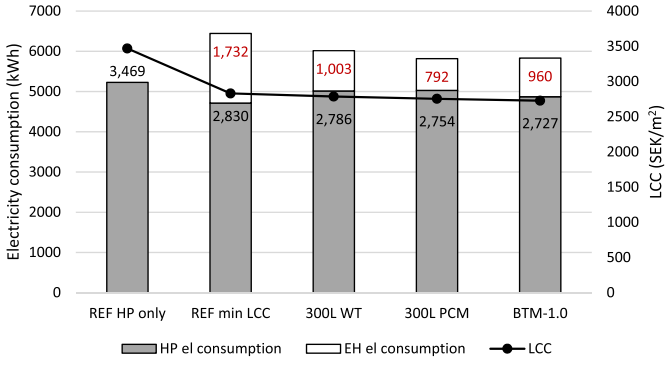

Fig. 8. Annual electricity consumptions and LCC for systems under day schedule. The electricity consumptions of EH are marked in red and the LCCs are marked in black.

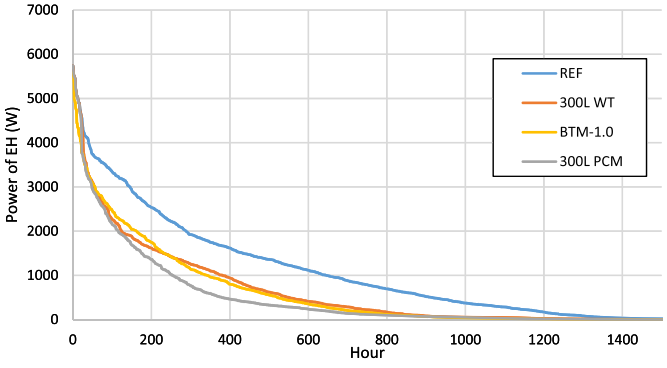

Fig. 9. EH power duration curve for the REF scenario and three TES scenarios under the day schedule.

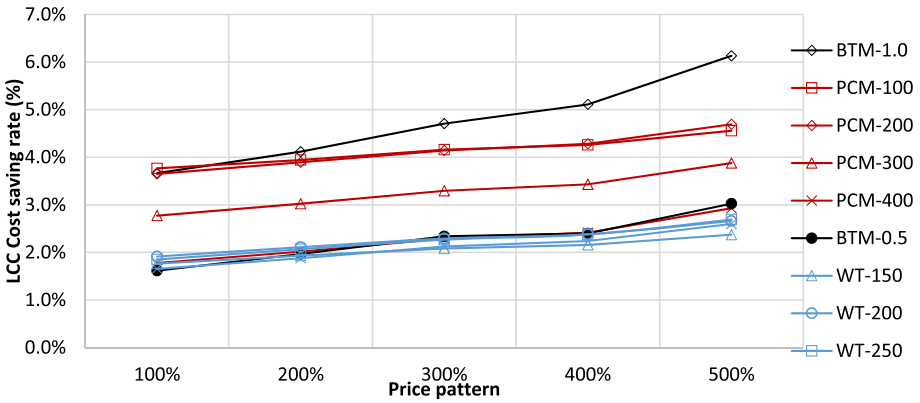

Fig. 10. LCC saving for investigated systems applied in SFH1 under day operating schedule.

peak usage of EH, as explained above. The remaining benefit from load shifting to a lower price period only contributes with a small part in the total economical saving and cannot offset the additional cost for the increased heat losses. For the cases with a larger variable price pattern, the economical saving from peak reduction is reduced while the saving from load shifting is increased. This is due to that the difference between peak EH cost and high operation cost of HP is smaller when the price has larger variations. Besides, compared to the WT, the PCM has smaller heat losses and higher discharge efficiency, due to its compact design and high storage density. Indeed, based on the empirical investment data and designed temperature difference, the equivalent investment per storage capacity for WT and PCM tank is 721 SEK/kWh and 385 SEK/kWh, respectively. As for the BTM system, the benefit from peak reduction and load shifting is increasing accordingly with the designed temperature deviation range. However, the equivalent heat loss is a positive value in the BTM system because the average indoor and outdoor air temperature difference is slightly reduced by the optimal control, while the average indoor air temperature is still kept at 20 °C. A summary of the KPIs of the optimal system under day schedule is presented in Table 9.

3.2. SFH1 under stable schedule

The annual electricity consumptions and LCC for SFH1 systems operated under the stable schedule are shown in Fig. 12. Similar as the analysis in Section 3.1, the volume of 300 L is used as an example for the WT and PCM. Compared to the results presented in Fig. 8, the peak reduction benefits are limited in the stable schedule.

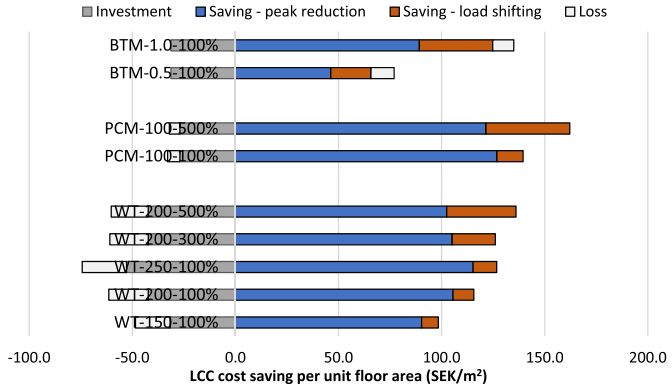

Fig. 11. Breakdown analysis of LCC saving for selected systems under day schedule. Short name: TES type-Size-Price.

This is explained by that the EH is only used during the coldest period, which creates little space for peak load shifting since the heat pump is already operated at the maximum capacity during that period. As can see in the REF scenario, the peak EH demand is reduced from 1732 kWh under day schedule to 603 kWh under stable schedule. Associated with this, the economic benefits are hugely reduced in the stable schedule. Due to the additional investments associated with the TES units, the three investigated TES systems all present larger LCC compared to the REF scenario designed with the minimal LCC. Further explanations on the economic benefits are illustrated in Fig. 14, based on breakdown analysis.

The performances of TES systems under different storage options and price patterns were also modelled. As shown in Fig. 13, under all price patterns, the LCC for the WT and PCM tank are higher than the REF scenario. However, the minimal LCC is still achieved at the volume of 200 L and 100 L, for the WT and PCM tank respectively. As for the BTM, the LCC saving is only positive when the variable price is larger than 300%. A similar LCC saving breakdown analysis is conducted and the results are shown in Fig. 14. Without the benefit from cost reduction, the benefit from load shifting cannot offset the investment and thermal losses.

The practical discharge efficiency for the WT and PCM under optimal size are 85% and 96%, respectively. Indeed, the annual heat loss for a 200 L WT is 172 kWh, which corresponds to 49 kWh electricity usage and an equivalent cost of 75 SEK if calculated for the design COP and average price. However, the annual discharge energy from this WT is only 1007 kWh. A theoretical hypothesis can be assumed that all discharged energy is used to shift the load from the highest price to the lowest price. Then, based on the current prices provided in Table 8, a theoretical maximum cost saving from load shifting is calculated as 57.5 SEK, which is still smaller than the cost for the corresponding heat losses. In fact, the daily maximum price might only continue for a short period like 1 h. The practical cost-saving is hardly the same as the theoretical maximum saving, giving that the discharge power is restricted. The above analysis also explains why the PCM tank has better economic performance than the WT in the small-scale application.

3.3. Influence of building insulation levels

Based on the methodologies for selecting the LCC optimal HP size and TES size, similar simulations were performed in SFH2 and SFH3, to provide a comprehensive performance of TES options under different buildings. The selected LCC optimal designs of TES systems for comparison are listed in Table 11, which represents the lowest LCC design.

Table 9
Performance of optimal systems under current price pattern and day schedule in SFH1. Q and E refer to the accumulated heat and electricity consumption, respectively.

System	Storage capacity (kWh)	Q-HP (kWh)	Q-EH (kWh)	E-total (kWh)	Q-Charge (kWh)	Q-Discharge (kWh)	C_{inv} (SEK/m^2)	$C_{elop} + C_{O\&M}$ (SEK/m^2)	C_{tot} (SEK/m^2)
REF	–	16,513	1732	6444	0	0	1110	1723	2833
WT-200	4.7	17,410	1098	6067	1747	1460	1152	1626	2779 (−1.9%)
PCM-100	5.6	17,326	971	5915	1239	1151	1137	1589	2726 (−3.8%)
BTM-1.0	8.4	17,096	960	5830	2371	2525	1176	1550	2727 (−3.7%)

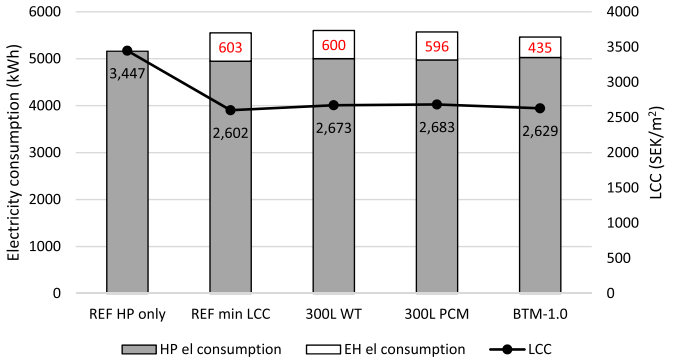

Fig. 12. Annual electricity consumptions and LCC for systems under stable schedule. The electricity consumptions of EH are marked in red and the LCCs are marked in black.

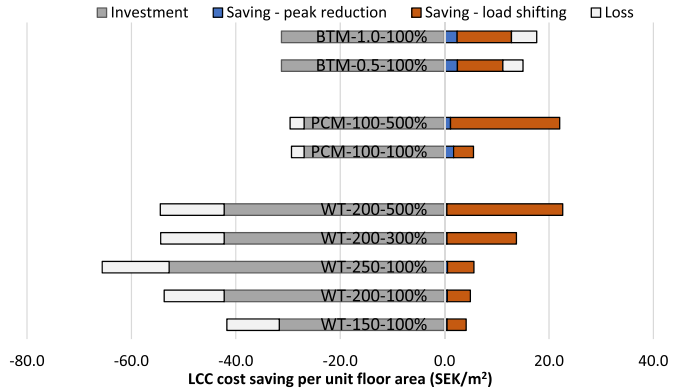

Fig. 14. Breakdown of LCC saving for selected systems under stable schedule. Short name: TES type-Size-Price.

The breakdown results of LCC savings under the day schedule and the current 100% price are presented in Fig. 15. Each bar represents the optimal system design under a certain TES option and a building insulation level. The LCC saving for the WT system is less than the PCM or BTM system. When comparing the performance of the three buildings, the absolute value of the LCC saving becomes smaller when the building has a higher insulation level. This can be explained by the smaller designed HP capacity and charging power in better-insulated buildings. However, the total LCC C_{tot} is also reduced in SFH3, thus the LCC saving rate remains relatively stable.

As for the BTM systems, the LCC saving is also smaller in better-insulated buildings. This conclusion differs from the previous understanding of the BTM, i.e. that better-insulated buildings have larger time constant and better thermal autonomy [30]. Several reasons can explain this phenomenon:

1) In buildings with larger time constant, the entire heating system can be shut down for a longer period before reaching the limit of thermal comfort. However, in real cases with timely variable electricity prices, the desired shut down period only lasts for around 1–3 h. With a decreasing heating power in better-insulated buildings, only limited energy can be discharged from the building mass within a given period. The potential of BTM is, therefore, hard to be fully utilized.
2) One control principle of the BTM in this study is to keep the average temperature at 20 °C. Thus, the investigated benefit only comes from the peak reduction and load shifting. Indeed, it is possible for the heating systems to be shut down for a longer period to decrease the average temperature, which belongs to an energy-saving measure. This measure is currently not considered in order not to create a prejudicial comparison among TES options.

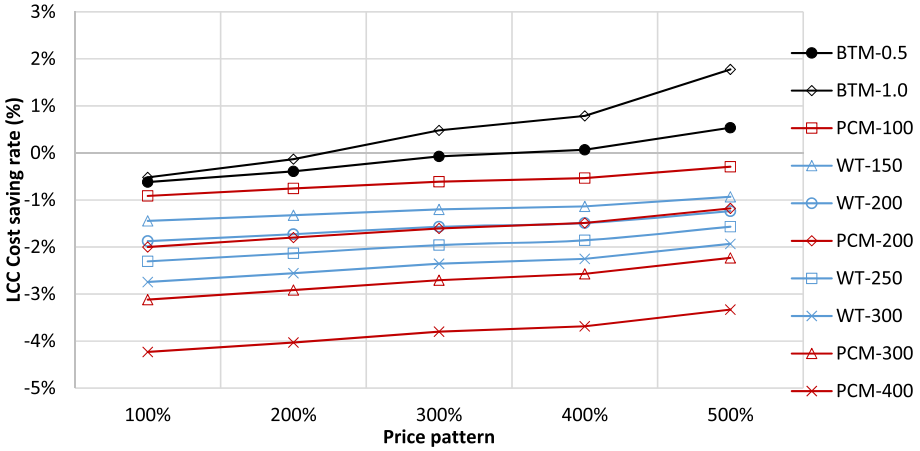

Fig. 13. LCC saving for investigated systems under stable schedule in SFH1.

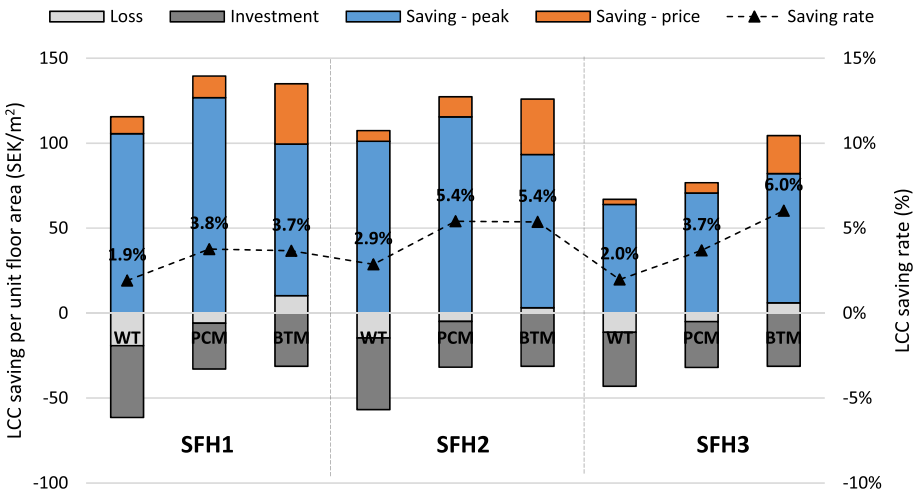

Fig. 15. Economic performance of three buildings with optimal TES design under day schedule and current 100% price.

Thus, from the simulation results, the less insulated buildings might enjoy more LCC saving from the utilization of BTM. However, the relative saving rate in SFH3 is higher due to a smaller total LCC. This conclusion is in line with previous research on the flexibility of different buildings in Denmark [27] and TES options in the whole Danish energy system [15].

The discharge performances of investigated systems are illustrated in Fig. 16. An index called equivalent cycle (EC) is calculated by dividing the discharged energy by the nominal storage capacity, which reflects the number of discharge cycles along the simulated year. Compared to a WT, a PCM tank has a smaller EC under the same system design, due to that it has lower discharge power. This can also be observed from results in Tables 9 and 10, where a PCM tank with higher storage capacity is utilized less often than a smaller WT. However, for the BTM, the discharge performance is highly restricted by the building load. As explained above, due to a decreasing average heat power demand in SFH2 and SFH3, the storage capacity is seldom fully utilized. Thus, EC become smaller for SFH2 and SFH3 than for SFH1.

Applying similar methods, the results for optimal TES options under the stable schedule are shown in Fig. 17. As is discussed in Section 3.2, without the benefit from peak reduction, the LCC for all TES options are higher than the REF scenario. A similar trend about the influence of building physics is also observed in the stable schedule. Although the LCC becomes higher after applying TES options, the WT tank and the PCM tank can shift approximately 13% of the annual heat demand while the BTM can shift more, i.e., 20% of the annual demand in SFH3. This means, if there exists a price with larger variable part or other cheap renewable energy sources such as solar power, it is still possible for TES options to have a positive LCC saving even under the stable schedule.

4. Discussion

The modelled results and calculated benefits for utilizing the household TES unit vary significantly among investigated scenarios. To achieve a positive payback, the initial investment of TES shall be covered by economic benefits from flexible operation. Considering an average COP of 3.5 and an average electricity price of 1.52 SEK/kWh, the operation cost for the GSHP and EH to supply unit amount of heat are 0.43 SEK/kWh and 1.52 SEK/kWh, respectively. Under day operating schedule, the heat price difference is 1.09 SEK/kWh, which is the driving force for the peak reduction by TES. However, under the stable operating schedule, even with a 500% amplified price pattern, the daily average price difference of electricity is 1.01 SEK/kWh, as shown in Table 8. Considering the same COP value, the

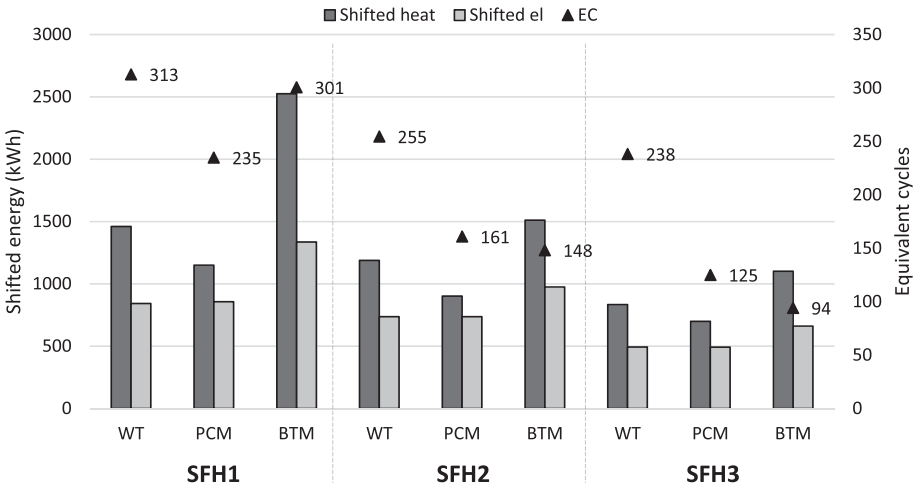

Fig. 16. Discharge performance of three building systems with optimal TES design under day schedule.

Table 10
Performance of optimal systems under current price pattern and stable schedule. Q and E represent same variables as in Table 9.

System	Storage capacity	Q-HP	Q-EH	E-total	Q-Charge	Q-Discharge	C_{inv}	$C_{elop} + C_{O\&M}$	C_{tot}
	(kWh)	(kWh)	(kWh)	(kWh)	(kWh)	(kWh)	(SEK/m^2)	(SEK/m^2)	(SEK/m^2)
REF	–	17367	603	5551	0	0	1110	1492	2602
WT-200	4.7	17524	600	5592	1179	1007	1152	1498	2651 (+1.9%)
PCM-100	5.6	17406	593	5552	1062	1025	1137	1489	2626 (+0.9%)
BTM-1.0	8.4	17487	592	5563	1994	2067	1176	1440	2616 (+0.5%)

Table 11
Optimal design parameters of TES systems for comparison between three buildings.

Buildings	Max heating load (kW)	Heating source		TES options		
		HP (kW)	EH (kW)	WT (m^3)	PCM (m^3)	BTM (°C)
SFH1	10	4.2	5.8	0.2	0.1	1
SFH2	7	2.4	4.6	0.2	0.1	1
SFH3	5.5	2	3.5	0.15	0.1	1

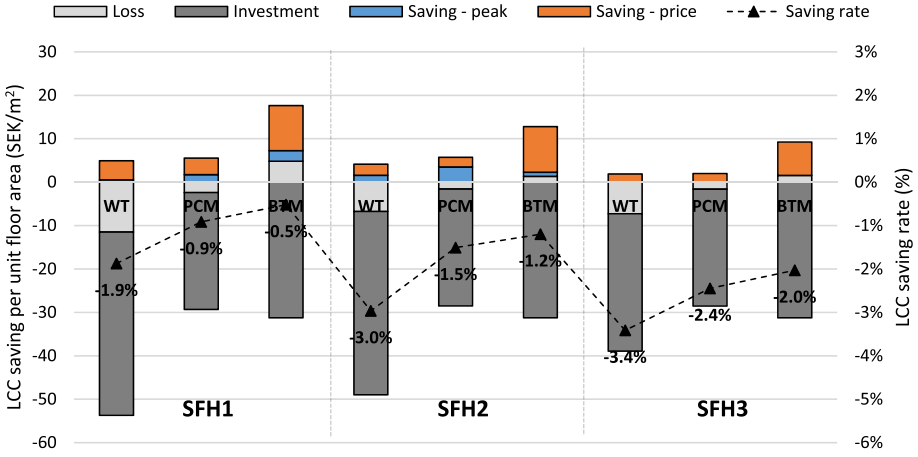

Fig. 17. Economic performance of the three buildings with optimal TES design, under the stable schedule and the current 100% price.

heat price difference is only 0.29 SEK/kWh. Considering the practical issues such as heat losses, the price difference and the associated benefits in stable schedule can hardly motivate the economic choice of TES. With the knowledge of energy profiles and prices, a simple and straightforward analysis method, as discussed above, can be applied to pre-identify the economic driving forces for utilizing the TES. Based on that, maximum economic potentials from TES can be further identified, which are relevant for future cost-optimal applications of household TES technologies.

Certain limitations still exist in the HP models, PCM models and the optimization process. The HP model used is a simplified empirical model. Limited by the function of the HP model, the start-up cost due to inevitable cycling loss for HP is seldom considered [59]. Meanwhile, the COP is also influenced positively in partial load conditions. A recent study [59] has summarized the current typical model simplifications for HP systems and investigated the influence of modelling complexities on the system performance. Thus, an improved model of HP is recommended to better depict the performance of the TES integrated energy system.

This study used a one-dimensional modelling approach to describe the heat and mass transfer dynamics of WT and PCM tanks in a rather simplified way. As for the PCM tank, a shell-and-tube structure is applied, with design parameters derived from previous studies [18]. However, there are certain points overlooked in this model. First, the performance of PCM can be further enhanced by several measures like the use of fins to enhance thermal conductivity, as summarized in Ref. [60]. Accordingly, new investment is also needed. The PCM's price used is consistent with its basic structure. Second, practical issues such as supercooling [61] and material fatigue is not considered, which might influence the economic benefit.

Another simplification made in this study is the optimization time span. Due to the difficulty of solving non-linear problems only daily optimization with a control step of 1 h is applied, which might influence the results when there are dramatic changes in electricity prices and heating load during short sections of days. In previous research works with simplified TES models [8], the whole system is linearized so optimizations in the annual time span can be conducted based on linear programming. However, the weather in Nordic countries is relatively stable in winter, which reduces the influence of the optimization time step.

5. Conclusion

In this study, the energy performance and economic benefit were considered and compared for three typical TES technologies applied in three cases of a Swedish SFH. Special focuses were paid on the differences between the TES technologies in the low-temperature range and the factors that influence the cost-effectiveness of the entire heating system. Different variables

including operating schedules, TES sizes, and variable electricity prices are combined and investigated. Besides, the thermal losses and practical discharge performances under limited heating power were better explained, which gives more realistic meanings to the TES options. Based on the simulation results under various conditions, following conclusions are made:

1) The major economic benefit for installing TES comes from the reduced usage of peak capacity, which is EH in this study. Buildings with varying temperature setpoint schedules and daily peak load profiles are found to have LCC saving potentials between 2% and 5% under the current electricity price, while the buildings with a stable schedule have almost no benefit from the peak reduction, which gives a negative LCC saving.
2) Comparing TES options for DSM, the WT is found to be less cost-effective than the PCM tank and the BTM due to high thermal losses and a low storage density in the low temperature range. However, the discharge performance alone for the WT is better than of the PCM tank because the latter has lower discharge power due to the low thermal conductivity of the material. As for the BTM, the condition with a 1 K temperature deviation can generate the highest LCC saving among all TES options.
3) In buildings with higher degree of insulation and lower thermal losses, the charging and discharging power of the TES is restricted, which causes less practical discharged energy and cost savings compared to baseline poorly insulated buildings. However, the cost-saving rate remains basically the same because the LCC of equipment is also smaller in the renovated buildings.
4) With the current variable electricity price in Sweden, it is hard to motivate investments in household WT and PCM tanks under stable operating schedule. The BTM has better economic performance than the two other active TES options since a smaller investment is needed. Thus, it shall be firstly considered for a DSM. However, the economically optimal TES options can shift around 10% of the total heat consumption and 10% of the electricity consumption. If additional prices or policies are implemented, there may be more incentives for the residents to invest in household active TES options.

Credit author statement

Yichi Zhang: Methodology, Validation, Investigation, Formal analysis, Writing – original draft, Pär Johansson: Conceptualization, Writing – review & editing, Supervision, Angela Sasic Kalagasidis: Conceptualization, Resources, Writing – review & editing, Supervision.

Declaration of competing interest

The authors declare that they have no known competing financial interests or personal relationships that could have appeared to influence the work reported in this paper.

Acknowledgement

This work was supported by the Swedish Research Council for Environment, Agricultural Sciences and Spatial Planning (FORMAS) [Grant No. 2018-01228].

Appendix. Radiator model

A one-dimensional air-water heat exchanger model with 10 nodes along the water flow direction is applied [62]. For each node, the energy balance equation reads as Appendix Eq. (1). K_r (W/(m^2·K)) denotes the equivalent heat transfer coefficient, which is in exponential relationship with the temperature difference between the water and the air [63], as noted in Appendix Eq. (2).

$$\rho V C_r \frac{\partial T_r}{\partial t} = u \rho C_p \frac{\partial T_r}{\partial x} - K_r A (T_r - T_a) \quad (\mathrm{W}) \tag{1a}$$

$$\frac{K_r}{K_{r,0}} = \left(\frac{T_r - T_a}{T_{r,0} - T_{a,0}} \right)^{1.3} \quad (-) \tag{2a}$$

where T_r (°C) represents the temperature of radiator node and T_a (°C) is the indoor air temperature. The variables $K_{r,0}$, $T_{r,0}$, and $T_{a,0}$ (W/(m^2·K)), represent the value in design condition.

References

[1] Pursiheimo E, Holttinen H, Koljonen T. Path toward 100% renewable energy future and feasibility of power-to-gas technology in Nordic countries. IET Renew Power Gener 2017;11:1695–706. https://doi.org/10.1049/iet-rpg.2017.0021.
[2] European Commission. The future role and challenges of Energy Storage. DG ENER Work Pap 2013:1–36.
[3] Fischer D, Madani H. On heat pumps in smart grids: a review. Renew Sustain Energy Rev 2017;70:342–57. https://doi.org/10.1016/j.rser.2016.11.182.
[4] The Swedish Energy Agency. Energistatistik for Småhus 2018. Energimyndigheten; 2019.
[5] Kohlhepp P, Harb H, Wolisz H, Waczowicz S, Müller D, Hagenmeyer V. Large-scale grid integration of residential thermal energy storages as demand-side flexibility resource: a review of international field studies. Renew Sustain Energy Rev 2019;101:527–47. https://doi.org/10.1016/j.rser.2018.09.045.
[6] Hewitt NJ. Heat pumps and energy storage - the challenges of implementation. Appl Energy 2012;89:37–44. https://doi.org/10.1016/j.apenergy.2010.12.028.
[7] Heier J, Bales C, Martin V. Combining thermal energy storage with buildings - a review. Renew Sustain Energy Rev 2015;42:1305–25. https://doi.org/10.1016/j.rser.2014.11.031.
[8] Fischer D, Lindberg KB, Madani H, Wittwer C. Impact of PV and variable prices on optimal system sizing for heat pumps and thermal storage. Energy Build 2016;128:723–33. https://doi.org/10.1016/j.enbuild.2016.07.008.
[9] Alimohammadisagvand B, Jokisalo J, Kilpeläinen S, Ali M, Sirén K. Cost-optimal thermal energy storage system for a residential building with heat pump heating and demand response control. Appl Energy 2016;174:275–87. https://doi.org/10.1016/j.apenergy.2016.04.013.
[10] Renaldi R, Kiprakis A, Friedrich D. An optimisation framework for thermal energy storage integration in a residential heat pump heating system. Appl Energy 2017;186:520–9. https://doi.org/10.1016/j.apenergy.2016.02.067.
[11] Lizana J, Friedrich D, Renaldi R, Chacartegui R. Energy flexible building through smart demand-side management and latent heat storage. Appl Energy 2018;230:471–85. https://doi.org/10.1016/j.apenergy.2018.08.065.
[12] Reynders G, Nuytten T, Saelens D. Potential of structural thermal mass for demand-side management in dwellings. Build Environ 2013;64:187–99. https://doi.org/10.1016/j.buildenv.2013.03.010.
[13] Péan TQ, Ortiz J, Salom J. Impact of demand-side management on thermal comfort and energy costs in a residential nZEB. Buildings 2017;7:1–19. https://doi.org/10.3390/buildings7020037.
[14] Hu M, Xiao F, Jørgensen JB, Li R. Price-responsive model predictive control of floor heating systems for demand response using building thermal mass. Appl Therm Eng 2019;153:316–29. https://doi.org/10.1016/j.applthermaleng.2019.02.107.
[15] Hedegaard K, Balyk O. Energy system investment model incorporating heat pumps with thermal storage in buildings and buffer tanks. Energy 2013;63:356–65. https://doi.org/10.1016/j.energy.2013.09.061.
[16] Hedegaard K, Mathiesen BV, Lund H, Heiselberg P. Wind power integration using individual heat pumps - analysis of different heat storage options. Energy 2012;47:284–93. https://doi.org/10.1016/j.energy.2012.09.030.
[17] Schibuola L, Scarpa M, Tambani C. Demand response management by means of heat pumps controlled via real time pricing. Energy Build 2015;90:15–28. https://doi.org/10.1016/j.enbuild.2014.12.047.
[18] Finck C, Li R, Kramer R, Zeiler W. Quantifying demand flexibility of power-to-heat and thermal energy storage in the control of building heating systems. Appl Energy 2018;209:409–25. https://doi.org/10.1016/j.apenergy.2017.11.036.
[19] Verhelst C, Logist F, Van Impe J, Helsen L. Study of the optimal control problem formulation for modulating air-to-water heat pumps connected to a residential floor heating system. Energy Build 2012;45:43–53. https://doi.org/10.1016/j.enbuild.2011.10.015.
[20] Søgaard R, Vad B, Reinert U, William D. Heat Roadmap Sweden. 2018.
[21] Lund H, Østergaard PA, Connolly D, Mathiesen BV. Energy storage and smart

energy systems. Energy 2017;137:556–65. https://doi.org/10.1016/j.energy.2017.05.123.
[22] Tan P, Lindberg P, Eichler K, Löveryd P, Johansson P, Kalagasidis AS. Thermal energy storage using phase change materials: techno-economic evaluation of a cold storage installation in an office building. Appl Energy 2020;276:115433. https://doi.org/10.1016/j.apenergy.2020.115433.
[23] Reynders G, Diriken J, Saelens D. Generic characterization method for energy flexibility: applied to structural thermal storage in residential buildings. Appl Energy 2017;198:192–202. https://doi.org/10.1016/j.apenergy.2017.04.061.
[24] Clauß J, Finck C, Vogler-finck P, Beagon P. Control strategies for building energy systems to unlock demand side flexibility – a review Norwegian University of Science and technology , Trondheim , Norway Eindhoven University of technology , Eindhoven , Netherlands Neogrid technologies ApS/Aalborg. 15th Int Conf Int Build Perform 2017;20:611.
[25] Le Dréau J, Heiselberg P. Energy flexibility of residential buildings using short term heat storage in the thermal mass. Energy 2016;111:991–1002. https://doi.org/10.1016/j.energy.2016.05.076.
[26] Johra H, Heiselberg P, Dréau J Le. Influence of envelope, structural thermal mass and indoor content on the building heating energy flexibility. Energy Build 2019;183:325–39. https://doi.org/10.1016/j.enbuild.2018.11.012.
[27] Foteinaki K, Li R, Heller A, Rode C. Heating system energy flexibility of low-energy residential buildings. Energy Build 2018;180:95–108. https://doi.org/10.1016/j.enbuild.2018.09.030.
[28] Foteinaki K, Li R, Péan T, Rode C, Salom J. Evaluation of energy flexibility of low-energy residential buildings connected to district heating. Energy Build 2020;213:109804. https://doi.org/10.1016/j.enbuild.2020.109804.
[29] Kensby J, Trüschel A, Dalenbäck JO. Potential of residential buildings as thermal energy storage in district heating systems - results from a pilot test. Appl Energy 2015;137:773–81. https://doi.org/10.1016/j.apenergy.2014.07.026.
[30] Intelligence Energy Europe Project TABULA. National building typologies database. 2021. https://episcope.eu/building-typology/.
[31] Antonopoulos KA, Koronaki E. Envelope and indoor thermal capacitance of buildings. Appl Therm Eng 1999;19:743–56. https://doi.org/10.1016/S1359-4311(98)00080-5.
[32] De Wit MH, Driessen HH. ELAN-A computer model for building energy design. Build Environ 1988;23:285–9. https://doi.org/10.1016/0360-1323(88)90034-0.
[33] De Wit MH, Driessen HH, van der Velden RMM. ELAN, a computermodel for building energy design: theory and validation. Faculteit der Bouwkunde; 1987. Technische Universiteit.
[34] Ics E. Svensk STANDARD SS-EN ISO 52016-1:2017. 2012.
[35] Wang A, Li R, You S. Development of a data driven approach to explore the energy flexibility potential of building clusters. Appl Energy 2018;232:89–100. https://doi.org/10.1016/j.apenergy.2018.09.187.
[36] de Normalización CE. EN ISO 13790: energy performance of buildings: calculation of energy use for space heating and cooling. CEN; 2008. ISO 13790:2008.
[37] SFS-EN 15316-3-1. Heating systems in buildings — method for calculation of system energy requirements and system efficiencies — Part 3-1 Domestic hot water systems , characterisation of needs (tapping requirements). 2006. p. 1–20.
[38] Ahmed K, Pylsy P, Kurnitski J. Monthly domestic hot water profiles for energy calculation in Finnish apartment buildings. Energy Build 2015;97:77–85. https://doi.org/10.1016/j.enbuild.2015.03.051.
[39] Lund H, Werner S, Wiltshire R, Svendsen S, Eric J, Hvelplund F, et al. 4th Generation District Heating (4GDH) Integrating smart thermal grids into future sustainable energy systems. Energy 2014;68:1–11. https://doi.org/10.1016/j.energy.2014.02.089.
[40] Best I, Braas H, Orozaliev J, Jordan U, Vajen K. Systematic investigation of building energy efficiency standard and hot water preparation systems' influence on the heat load profile of districts. Energy 2020;197:1–12. https://doi.org/10.1016/j.energy.2020.117169.
[41] Yang X, Li H, Svendsen S. Energy, economy and exergy evaluations of the solutions for supplying domestic hot water from low-temperature district heating in Denmark. Energy Convers Manag 2016;122:142–52. https://doi.org/10.1016/j.enconman.2016.05.057.
[42] Sweden S. Electricity supply, district heating and supply of natural gas. 2015. Stat Medd EN11SM1601 2016.
[43] Zhang Y, Campana PE, Yang Y, Stridh B, Lundblad A, Yan J. Energy flexibility from the consumer: integrating local electricity and heat supplies in a building. Appl Energy 2018;223:430–42. https://doi.org/10.1016/j.apenergy.2018.04.041.
[44] Cruickshank CA, Harrison SJ. Heat loss characteristics for a typical solar domestic hot water storage. Energy Build 2010;42:1703–10. https://doi.org/10.1016/j.enbuild.2010.04.013.
[45] Li P, Van Lew J, Chan C, Karaki W, Stephens J, O'Brien JE. Similarity and generalized analysis of efficiencies of thermal energy storage systems. Renew Energy 2012;39:388–402. https://doi.org/10.1016/j.renene.2011.08.032.
[46] Colella F, Sciacovelli A, Verda V. Numerical analysis of a medium scale latent energy storage unit for district heating systems. Energy 2011;45:2455–68. https://doi.org/10.1016/j.energy.2012.03.043.
[47] Belusko M, Halawa E, Bruno F. Characterising PCM thermal storage systems using the effectiveness-NTU approach. Int J Heat Mass Tran 2012;55:3359–65. https://doi.org/10.1016/j.ijheatmasstransfer.2012.03.018.
[48] Tay NHS, Belusko M, Bruno F. An effectiveness-NTU technique for characterising tube-in-tank phase change thermal energy storage systems. Appl Energy 2012;91:309–19. https://doi.org/10.1016/j.apenergy.2011.09.039.
[49] Agyenim F, Hewitt N, Eames P, Smyth M. A review of materials, heat transfer and phase change problem formulation for latent heat thermal energy storage systems (LHTESS). Renew Sustain Energy Rev 2010;14:615–28. https://doi.org/10.1016/j.rser.2009.10.015.
[50] Sweden interest rates. http://sweden.deposits.org. [Accessed 13 October 2020].
[51] Kuboth S, Heberle F, König-Haagen A, Brüggemann D. Economic model predictive control of combined thermal and electric residential building energy systems. Appl Energy 2019;240:372–85. https://doi.org/10.1016/j.apenergy.2019.01.097.
[52] Le Digabel S. Algorithm 909: NOMAD: Nonlinear optimization with the MADS algorithm. ACM Trans Math Software 2011;37:1–15.
[53] Currie J, Wilson DI, Sahinidis N, Pinto J. OPTI: lowering the barrier between open source optimizers and the industrial MATLAB user. Found Comput Process Oper 2012;24:32.
[54] Sommerfeldt N, Madani H. Ground source heat pumps for Swedish multi-family houses: innovative co-generation and thermal storage strategies (Effsys Expand final report). http://effsysexpand.se/wp-content/uploads/2018/09/EffsysExpandP21-FinalReport_Reviewed.pdf 2018.
[55] Espagnet AR. Techno-economic assessment of thermal energy storage integration into low temperature district heating networks. 2016. p. 94.
[56] Ekström T. Passive house renovation of Swedish single-family houses from the 1960s and 1970s. Lund University; 2017.
[57] Iso E. 7730. Ergon therm environ determ interpret therm comf using calc PMV PPD indices local therm comf criteria 2005. 2005.
[58] NordPool Group. NordPool, the leading power market in Europe. NordPool; 2020. https://www.nordpoolgroup.com/. [Accessed 16 February 2020].
[59] Clauß J, Georges L. Model complexity of heat pump systems to investigate the building energy flexibility and guidelines for model implementation. Appl Energy 2019;255:113847. https://doi.org/10.1016/j.apenergy.2019.113847.
[60] Jegadheeswaran S, Pohekar SD. Performance enhancement in latent heat thermal storage system: a review. Renew Sustain Energy Rev 2009;13:2225–44. https://doi.org/10.1016/j.rser.2009.06.024.
[61] Tan P, Lindberg P, Eichler K, Löveryd P, Johansson P, Kalagasidis AS. Effect of phase separation and supercooling on the storage capacity in a commercial latent heat thermal energy storage: Experimental cycling of a salt hydrate PCM. J Energy Storage 2020;29:101266. https://doi.org/10.1016/j.est.2020.101266.
[62] Tahersima F, Stoustrup J, Rasmussen H, Nielsen PG. Thermal analysis of an HVAC system with TRV controlled hydronic radiator. IEEE Int Conf Autom Sci Eng CASE 2010;2010. https://doi.org/10.1109/COASE.2010.5584535. 2010:756–61.
[63] Hansen LH. Stochastic modelling of central heating systems. 1997.